多波长红光金刚石拉曼激光器

张亚凯[1,2]，陈　晖[1,2]，白振峣[3*]，庞亚军[1,2]，王雨雷[1,2]，吕志伟[1,2]，白振旭[1,2*]

(1. 河北工业大学 先进激光技术研究中心，天津 300401；
2. 河北省先进激光技术与装备重点实验室，天津 300401；
3. 中国科学院空天信息创新研究院，北京 100094)

摘　要： 全固态红光激光器在激光显示、全息存储以及医疗领域有着重要应用，其中多波长红光激光器还可用于差频产生太赫兹辐射。基于三阶非线性效应受激拉曼散射的拉曼激光器是一种突破粒子数反转激光器有限发射光谱制约进而拓展激光波长的有效手段，即能够将注入的单一波长泵浦光直接拓展至一个或几个全新波段。笔者团队研制了一台绿光泵浦的多波长级联金刚石拉曼激光器，利用波长为 532 nm、脉冲宽度为 11.43 ns 的激光作为泵浦源，通过将一阶 Stokes 黄橙光 (573 nm) 锁定在振荡器中，实现了红光波段的二阶、三阶和四阶 (620 nm、676 nm 和 743 nm) 级联拉曼激光输出，对应三个波长的脉冲宽度分别为 10.41、3.75、2.45 ns，总输出能量为 0.6 mJ，光光转换效率为 36.38%。结果表明，凭借金刚石晶体优异的光学特性和拉曼性质，可见光泵浦的金刚石拉曼激光器对于实现高功率全固态小型化多波长红光激光输出具有巨大潜力。

关键词： 拉曼激光；　金刚石；　多波长；　脉冲；　高功率

0　引　言

红光通常指可见光范围内波长在 620~780 nm 的区间，该波段的光谱在工业、科研和医疗等领域具有广泛的应用。其中作为一种"特殊"的光源，全固态多波长红光激光器不仅在激光彩色大屏幕显示、全息存储、激光打印、激光测量以及激光医疗等方面有着重要应用[1–3]，而且多波长特性也使其成为通过差频产生太赫兹光源的有效途径[4–5]。目前，常见的直接获得单一波长红光激光辐射的光源包括氦氖激光器、半导体激光器和掺 Pr[3+]等稀土离子的固体激光器等[6–7]。其中，半导体红光激光器的线宽和光束质量通常难以控制，尤其是针对获得短脉冲高能量激光输出方面尚无报道；目前，已报道的掺 Pr[3+]全固态红光激光器的输出功率仅为 8.14 W，其功率的提升主要受制于蓝光泵浦源的发展[8]。此外，将反转粒子增益介质发射谱的多个发射峰与二阶非线性效应相结合是产生多波长红光输出的有效方式[9]。2019 年，长春理工大学的郭阳阳等人利用 Nd:YAG 晶体的 1 319 nm 和 1 338 nm 两个发射谱与腔内倍频技术相结合，获得了 659.5、669 nm 双波长红光输出，当最大泵浦功率为 35 W 时，双波长激光器的输出功率为 1.35 W[10]。但是，由于基频光波长 1 319 、1 338 nm 并不是增益介质 Nd:YAG 的最强发射峰，因此最终获得红光的转换效率仅为 4.08%。

受激拉曼散射 (SRS) 是一种高强度的三阶非线性效应，具有波长转换灵活、自动相位匹配、光束净化等优点[11–13]。利用拉曼转换的级联频移特性是一种通过单一泵浦波长实现多波长输出的有效方

红外与激光工程

第 8 期　　www.irla.cn　　第 52 卷

法[14−18]。相较于传统的拉曼介质，金刚石晶体不但拥有已知晶体中最大的拉曼频移 (1 332 cm⁻¹)，而且具有超高热导率 (>2 000 W·m⁻¹·K⁻¹) 和极宽光谱透过范围 (>0.23 μm)[19−21]。基于 1 μm 泵浦的金刚石拉曼激光器在近红外波段已经实现了高效的级联拉曼输出[20−23]，并且结合腔内倍频技术，也已经实现了 620 nm 单一波长红光的输出。2019 年，澳大利亚麦考瑞大学的 Mildren 团队，利用 1 064 nm 泵浦源泵浦外腔金刚石拉曼振荡器，通过腔内 LBO 晶体倍频获得了稳态功率 38 W 的 620 nm 红光输出[24]。2022 年，中国科学院 Chen 等人采用相同的腔内倍频外腔拉曼振荡器，在重复频率 2 kHz 的情况下，获得了平均功率 750 mW 的 620 nm 红光输出，光光转换效率为 11.19%[25]。腔内倍频结构是一种提高转换效率的有效方式，但该结构同时也增加了整个光学系统的设计难度，尤其是倍频晶体相位匹配角度对工作波长的选择性使其难以实现高效率的多波长激光输出。

相比之下，金刚石在可见光波段有着更高的拉曼增益系数 (~50 GW/cm@532 nm[26]，~10 GW/cm @ 1 064 nm[27])。因此，利用常见且成熟的 532 nm 激光器泵浦金刚石晶体，有望在实现高效、高能量、高光束质量的多波长红光激光输出方面展现强大的优势。2009 年，澳大利亚麦考瑞大学 Mildren 团队，利用 532 nm 的纳秒脉冲激光泵浦外腔金刚石拉曼振荡器，实现了 573 nm 一阶和 620 nm 二阶的 Stokes 光

输出，总转换效率为 63.5%[28]。2021 年，天津理工大学 Hu 等人利用金刚石晶体获得了 620 nm 的二阶 Stokes 光，平均输出功率为 1.95 W，斜率效率为 22.8%，激光阈值仅为 1.5 W[29]。目前，围绕 532 nm 泵浦的一阶和级联的金刚石拉曼转换已有报道，但是如何有效跨过黄橙光波段，直接实现单一和多波长红光波段输出，至今尚无研究。

针对上述问题，文中搭建了一台可见光泵浦可直接实现多波长红光激光输出的金刚石拉曼激光器。泵浦源为 532 nm 倍频绿光纳秒脉冲激光器，在最大泵浦能量为 1738 μJ 下，有效在振荡器内实现了对一阶 (573 nm) 拉曼波长的锁定，直接获得了二阶 (620 nm)、三阶 (676 nm) 以及四阶 (743 nm) 级联拉曼转换的多波长红光激光输出，对应的脉宽分别为 10.41、3.75、2.45 ns，输出能量分别为 142.7、424.6、65.1 μJ，转换效率为 36.38%。

1　实验装置

多波长红光金刚石拉曼激光器结构如图 1 所示。其中，泵浦源为自主搭建的 532 nm 倍频脉冲激光器，其对应的最大泵浦能量为 1738 μJ，脉宽为 11.43 ns，重复频率为 1~500 Hz 可调。通过透镜组 F1、F2 对泵浦光进行整形准直，谐振腔前的二分之一波片 (HWP) 用于调节泵浦光的偏振方向使其平行于金刚石晶体的<111>轴，从而获得最大的拉曼增益[30]。
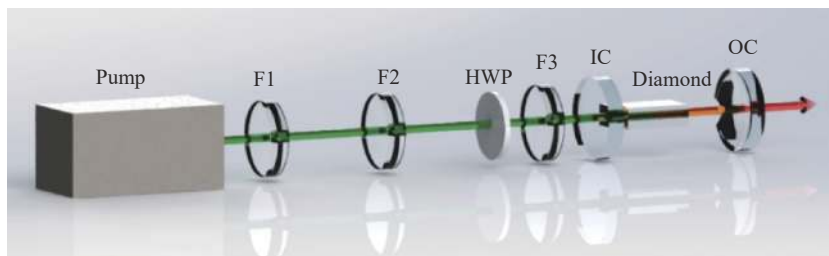

图 1　多波长红光金刚石拉曼激光器实验结构装置图

Fig.1　Experimental setup of multi-wavelength diamond Raman laser in red

为了提高腔内注入功率和避免腔内元件损伤，金刚石拉曼振荡器采用具有较大模式体积的平凹腔型，输出镜的曲率半径为 200 mm，金刚石的尺寸为 2 mm× 4 mm×7 mm，腔镜镀膜情况参考表 1。其中，为抑制黄橙光的输出进而提高级联拉曼的转换效率，输入镜

(IC) 和输出镜 (OC) 均镀有对一阶 Stokes 光 573 nm 的高反射膜。耦合透镜 F3 将金刚石晶体内的泵浦光半径控制在 350 μm 左右。得益于金刚石极大的导热系数，在低重复频率泵浦下，腔内模式几乎不受热效应影响。拉曼振荡器腔长约为 60 mm，平面镜到金刚石

的距离为 7 mm。拉曼腔的各阶 Stokes 光的本征模式如图 2 所示,紫色虚线之间为金刚石晶体,仿真结果显示腔内一阶至四阶 Stokes 光在金刚石区域的基横模半径依次为 128 μm、133 μm、139 μm 和 146 μm。

<p style="text-align:center">表 1 腔镜的镀膜参数</p>
<p style="text-align:center">Tab.1 Coating parameters of cavity mirrors</p>

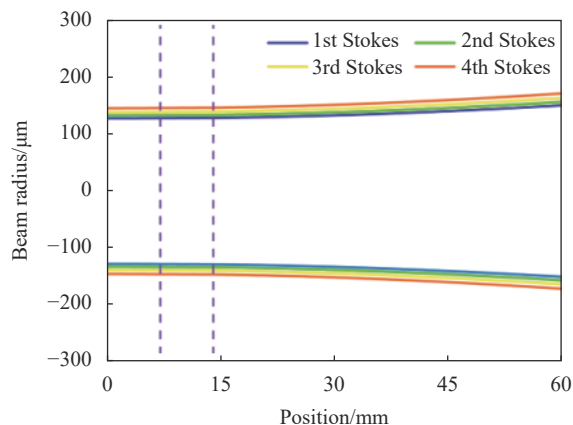|	Pump (532 nm)	First-Stokes (573 nm)	Second-Stokes (620 nm)	Third-Stokes (676 nm)	Fourth-Stokes (743 nm)
IC	AR	HR	HR	HR	R=87%
OC	HR	HR	R=10%	R=15%	R=69%

图 2 金刚石拉曼振荡器内各阶次 Stokes 光的基横模模式

Fig.2 The fundamental transverse modes of various Stokes orders in the diamond Raman oscillator

2 实验结果与分析

利用光纤光谱仪 (Toshiba 公司, 型号 TCD1304AP) 对不同泵浦功率下的输出光谱进行了采集,结果如图 3 所示。当泵浦能量为 343、437、1 165 μJ 时,分别采集到了二阶 Stokes 光、二阶和三阶 Stokes、二阶~四阶 Stokes 光的光谱信息,各阶 Stokes 光之间的频移为 1 332 cm^{-1},与金刚石晶体的理论拉曼频移值吻合。由于输出镜对一阶 Stokes 光为高反射率 (R>99.97%) 镀膜,所以并未在输出光中观察或采集到其任何光谱、能量信息,因此笔者有效实现了对一阶 573 nm 的黄橙光波长的抑制。

图 4 为利用不同截止波长的滤波片对各阶 Stokes 光能量测量的结果。随着泵浦能量增大,由于两腔镜镀有对一阶 Stokes 光的高反射率介质膜,腔内会形成高能量密度的一阶 Stokes 光场,从而提高泵浦光的耗尽率,并激发二阶 Stokes 光。当泵浦能量仅

为 200 μJ 时,肉眼观察到拉曼腔内出现波长为 573 nm 的一阶 Stokes 黄光振荡,但无激光输出。如图 4(a) 所示,二阶、三阶、四阶拉曼产生阈值分别为 343、437、1 165 μJ,在泵浦能量最大为 1 738 μJ 的情况下,获得了三波长能量分别为 142.7、424.6、65.1 μJ 的同时输出,对应的斜效率分别为 9.68%、31.29%、8.71%。波长为 743 nm 的四阶 Stokes 光相较于三阶 Stokes 光的阈值有较大的增长,其主要原因为输入镜对 743 nm 的反射率为 87%,腔内损耗较大。如图 4(b) 所示,随着泵浦能量的增加,总的光-光转换效率持续增加,最后趋于平缓。最终在泵浦能量最大为 1 738 μJ 的情况下,获得了共 632.4 μJ 的多波长红色激光输出,光-光转换效率为 36.38%。

采用光电探测器 (Thorlabs 公司, 型号 DET025A) 对入射拉曼腔的 532 nm 泵浦光和最大泵浦能量下输出的各阶 Stokes 光的时域波形进行了测量,结果如图 5 所示,其脉宽依次为 11.43、10.41、3.75、2.45 ns。
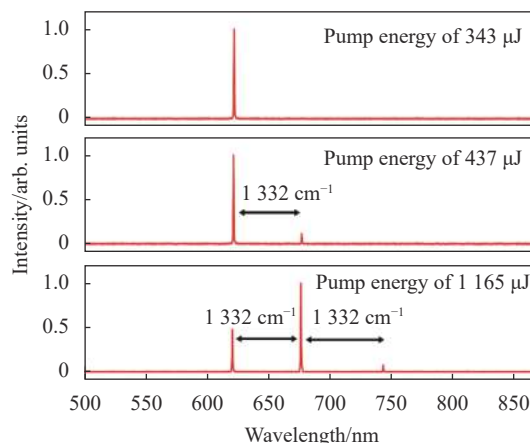

图 3 不同泵浦能量下金刚石级联拉曼激光器的输出光谱

Fig.3 Output laser spectra of diamond cascade Raman lasers at different pump energies
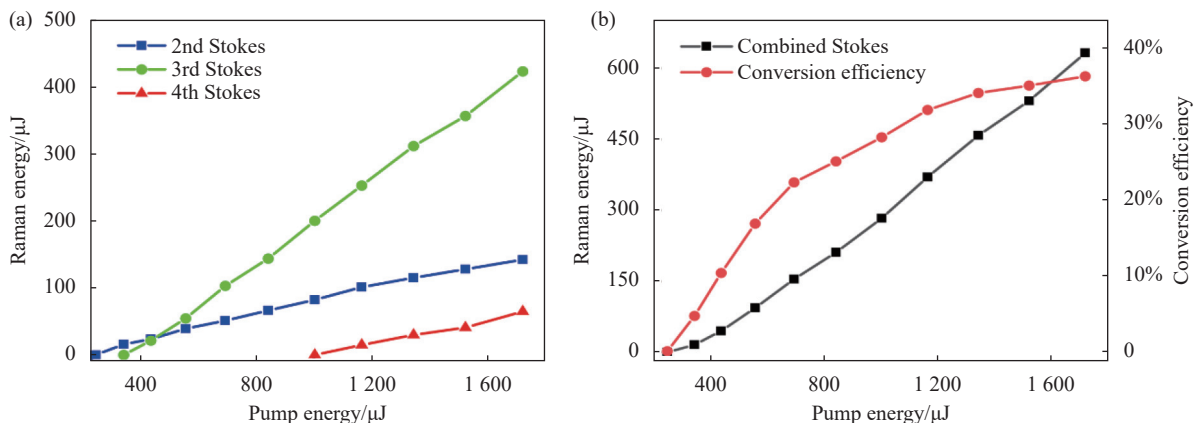
图 4 (a) 各波长 Stokes 光能量与泵浦能量关系图; (b) 总 Stokes 光能量、效率与泵浦能量关系图

Fig.4 (a) Stokes energy versus pump energy for each wavelength; (b) Total Stokes energy, efficiency versus pump energy
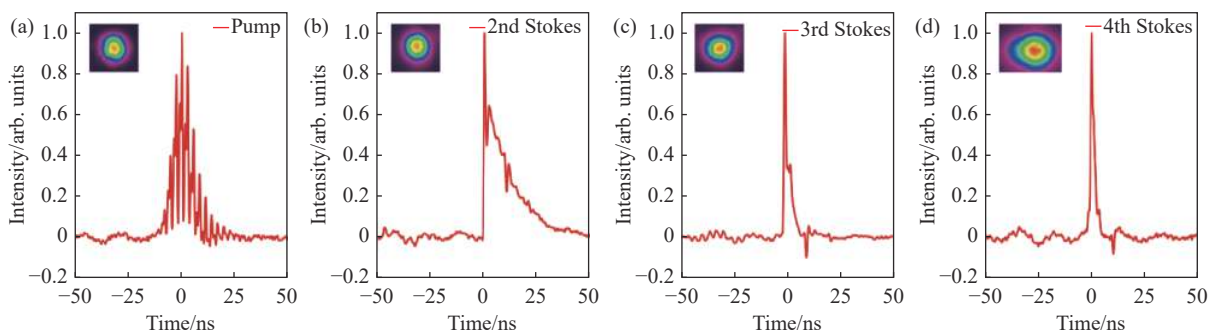

图 5 脉冲波形及光斑: (a) 泵浦光; (b) 二阶 Stokes 光; (c) 三阶 Stokes 光; (d) 四阶 Stokes 光

Fig.5 Temporal behavior and near-field spot : (a) Pump; (b) Second-order Stokes; (c) Third-order Stokes; (d) Fourth-order Stokes

根据测得的单脉冲能量计算得到产生的 620、676、743 nm 三阶红光的峰值功率分别为 12.5、40.8、17.4 kW。各阶 Stokes 光相较于泵浦光而言, 脉宽都得到了不同程度的压缩, 随着拉曼阶次的增加, 压缩效果越发明显。当腔内低阶 Stokes 光的能量密度达到高阶 Stokes 光的阈值时, 高阶 Stokes 光会耗尽低阶 Stokes 光的能量, 由此导致低阶 Stokes 光在波形上会出现中心高强度部分被耗尽, 剩下一个非常窄的前沿尖峰和一个后沿平台的现象, 其中 620 nm 脉冲波形中的前沿尖峰在百皮秒量级。如图 5 中的插图所示, 各阶 Stokes 光的近场光斑无明显畸变, 光斑形貌良好。

在上述实验中, 利用外腔拉曼振荡器实现了多波长红光激光输出, 并对其输出光谱、能量和空间分布特性进行了分析。该研究中, 金刚石晶体中心泵浦光的束腰半径为 Stokes 光的两倍以上, 未来通过优化泵浦光和腔内光束的模式匹配有望进一步提升其光光转换效率。此外, 该级联振荡器实现多波长输出的技术路线相比于光谱合成的方式, 能够直接实现多波长激光的同轴输出, 该特性使其在光电对抗、雷达探测等应用中拥有显著优势。

3 结 论

文中搭建了一台 532 nm 脉冲泵浦的金刚石拉曼激光器, 研究了不同泵浦能量下级联拉曼激光输出能量、光谱和脉冲特性, 最终成功实现了 620、676、743 nm 的级联拉曼输出。在泵浦能量最大为 1 738 μJ 的情况下, 620 nm 能量为 142.7 μJ, 676 nm 能量为 424.6 μJ, 743 nm 能量为 65.1 μJ, 测得了总共 632.4 μJ 的多波长红色激光输出, 光光转换效率为 36.38%。输出的各阶次拉曼激光脉冲宽度相对于泵浦光出现明显的压缩, 对应最大压缩比高达 4.7 倍 (11.43 ns@ 532 nm, 2.45 ns @743 nm), 且各阶 Stokes 光的近场光斑均具有较好的空间分布, 峰值功率均在 10 kW 以上。今后, 笔者将围绕振荡器腔镜参数的优化设计和输出光束整形开展深入研究, 进而实现精确调控各阶 Stokes 光的能量

以及提高多波长激光在空间的同步传输能力。综上所述，凭借极高的拉曼增益系数以及优良的光热性质，以金刚石晶体作为拉曼增益介质的可见光泵浦拉曼激光器，在实现高效的全固态小型化多波长高功率激光器方面具有巨大潜力。

参考文献：

[1] Ateş G B, Ak A, Garipcan B, et al. Methylene blue mediated photobiomodulation on human osteoblast cells [J]. *Lasers in Medical Science*, 2017, 32: 1847-1855.

[2] Núñez S C, França C M, Silva D F T, et al. The influence of red laser irradiation timeline on burn healing in rats [J]. *Lasers in Medical Science*, 2013, 28: 633-641.

[3] Chandran A, Battle R, Murray R, et al. Watt-level 743 nm source by second-harmonic generation of a cascaded phosphosilicate Raman fiber amplifier [J]. *Optics Express*, 2021, 29(25): 41467-41474.

[4] Li Yihan, Chen Shanzhuo, Guo Hao. Generation and application of multi-wavelength optical carriers based on stimulated Brillouin scattering [J]. *Chinese Journal of Lasers*, 2022, 49(19): 1906003. (in Chinese)

[5] Zhang Qiang, Yao Jianquan, Wen Wulin, et al. High power laser diode pumped Nd:YAG continuous wave dual-wavelength laser [J]. *Chinese Journal of Lasers*, 2006, 33(5): 577-581. (in Chinese)

[6] Huo Xiaowei, Qi Yaoyao, Li Yuqi, et al. Research progress of LD-pumped Pr^{3+}-doped solid-state laser in visible wavelength [J]. *Electro-Optic Technology Application*, 2019, 34(5): 7-15. (in Chinese)

[7] Xu Bin, Zhang Teng, Zou Jinhai, et al. Research progress of direct generation lasers in visible spectral range [J]. *Journal of Xiamen University (Natural Science)*, 2021, 60(3): 484-496. (in Chinese)

[8] Lin X, Chen M, Feng Q, et al. LD-pumped high-power CW Pr^{3+}: YLF Laguerre-Gaussian lasers at 639 nm [J]. *Optics & Laser Technology*, 2021, 142: 107273.

[9] Zhou H, Bi X, Zhu S, et al. Multi-wavelength passively Q-switched red lasers with Nd^{3+}:YAG/YAG/V^{3+}:YAG/YAG composite crystal [J]. *Optical and Quantum Electronics*, 2018, 50(2): 56.

[10] Guo Yangyang, Sun Rui, Jin Guangyong. Research on LBO frequency-double 659.5 nm/669 nm all-solid-state laser [J]. *Journal of Changchun University of Science and Technology*, 2019, 42(5): 9-12. (in Chinese)

[11] Bao Yushuo, Huang Haitao, Chen Haiwei, et al. 1.7 μm laser with a low frequency shifted Raman mode cascade connection [J]. *Infrared and Laser Engineering*, 2022, 51(7): 20210507. (in Chinese)

[12] Williams R J, Kitzler O, Bai Z, et al. High power diamond Raman lasers [J]. *IEEE Journal of Selected Topics in Quantum Electronics*, 2018, 24(5): 1602214.

[13] Bai Z, Williams R J, Jasbeer H, et al. Large brightness enhancement for quasi-continuous beams by diamond Raman laser conversion [J]. *Opt Lett*, 2018, 43(3): 563-566.

[14] Yang Ce, Chen Meng, Ma Ning, et al. Picosecond multi-pulse burst pump KGW infrared multi-wavelength Raman laser [J]. *Infrared and Laser Engineering*, 2020, 49(11): 20200044. (in Chinese)

[15] Granados E, Pask H M, Esposito E, et al. Multi-wavelength, all-solid-state, continuous wave mode locked picosecond Raman laser [J]. *Opt Express*, 2010, 18(5): 5289-5294.

[16] Lin H, Pan X, Huang X, et al. Multi-wavelength passively Q-switched c-cut Nd: YVO_4 self-Raman laser with Cr^{4+}:YAG saturable absorber [J]. *Optics Communications*, 2016, 368: 39-42.

[17] Frank M, Jelínek M, Vyhlídal D, et al. Multi-wavelength picosecond $BaWO_4$ Raman laser with long and short Raman shifts and 12-fold pulse shortening down to 3 ps at 1227 nm [J]. *Laser Physics*, 2018, 28(2): 025403.

[18] Zhang Ximei, Chen Simeng, Shi Shencheng, et al. Study on the performance of cascaded Nd:$GdVO_4$ self-Raman laser at 1 309 nm [J]. *Infrared and Laser Engineering*, 2019, 48(11): 1105002. (in Chinese)

[19] Bai Zhenxu, Chen Hui, Li Yuqi, et al. Development of beam brightness enhancement based on diamond Raman conversion [J]. *Infrared and Laser Engineering*, 2021, 50(1): 20200098. (in Chinese)

[20] Bai Zhenxu, Chen Hui, Zhang Zhanpeng, et al. Hundred-watt dual-wavelength diamond Raman laserat 1.2/1.5 μm (Invited) [J]. *Infrared and Laser Engineering*, 2021, 50(12): 20210685. (in Chinese)

[21] Bai Zhenxu, Yang Xuezong, Chen Hui, et al. Research progress of high-power diamond laser technology (Invited) [J]. *Infrared and Laser Engineering*, 2020, 49(12): 20201076. (in Chinese)

[22] Wang Y, Peng W, Yang X, et al. Efficient operation near the quantum limit in external cavity diamond Raman laser [J]. *Laser Physics*, 2020, 30(9): 095002.

[23] Li M, Kitzler O, Spence D J. Investigating single-longitudinal-

mode operation of a continuous wave second Stokes diamond Raman ring laser [J]. *Opt Express*, 2020, 28(2): 1738-1744.

[24]　Yang X, Kitzler O, Spence D J, et al. Single-frequency 620 nm diamond laser at high power, stabilized via harmonic self-suppression and spatial-hole-burning-free gain [J]. *Opt Lett*, 2019, 44(4): 839-842.

[25]　Chen Y, Liu J, Zhu X, et al. Intracavity frequency-doubled pulsed diamond Raman laser emitting at 620 nm [J]. *Appl Phys B*, 2022, 128(10): 186.

[26]　Spence D J, Granados E, Mildren R P. Mode-locked picosecond diamond Raman laser [J]. *Opt Lett*, 2010, 35(4): 556-558.

[27]　Sabella A, Piper J A, Mildren R P. Efficient conversion of a 1.064 μm Nd:YAG laser to the eye-safe region using a diamond Raman laser [J]. *Opt Express*, 2011, 19(23): 23554-23560.

[28]　Mildren R P, Sabella A. Highly efficient diamond Raman laser [J]. *Opt Lett*, 2009, 34(18): 2811-2813.

[29]　Tu H, Ma S, Hu Z, et al. Efficient monolithic diamond Raman yellow laser at 572.5 nm [J]. *Optical Materials*, 2021, 114: 110912.

[30]　Sabella A, Piper J A, Mildren R P. 1240 nm diamond Raman laser operating near the quantum limit [J]. *Opt Lett*, 2010, 35(23): 3874-3876.

Multi-wavelength red diamond Raman laser

Zhang Yakai[1,2]，Chen Hui[1,2]，Bai Zhenao[3*]，Pang Yajun[1,2]，Wang Yulei[1,2]，Lv Zhiwei[1,2]，Bai Zhenxu[1,2*]

(1. Center for Advanced Laser Technology, Hebei University of Technology, Tianjin 300401, China;

2. Hebei Key Laboratory of Advanced Laser Technology and Equipment, Tianjin 300401, China;

3. Aerospace Information Research Institute, Chinese Academy of Sciences, Beijing 100094, China)

Abstract:

Objective　The all-solid-state multi-wavelength red laser has significant applications in laser color large-screen displays, high-density holographic storage, measurement, and medical treatment. Its multi-wavelength characteristics also enable it to serve as a terahertz light source through difference-frequency generation. Currently, the multi-wavelength red laser can be generated by combining the emission spectrum of an inversion particle gain medium with second-order nonlinear effects. However, these methods typically have lower conversion efficiency. Stimulated Raman scattering (SRS) is a high-intensity third-order nonlinear effect that offers flexible wavelength conversion, automatic phase matching, and beam cleanup. The cascaded frequency shift property of Raman crystals is an effective method for achieving multi-wavelength output using a single pump wavelength. Diamond crystals have a high Raman gain coefficient in the visible wavelength range compared to conventional Raman crystals. Pumping diamond with a well-established 532 nm laser has great potential for obtaining efficient, high-energy, high-beam quality multi-wavelength red laser output. In this study, we investigate the generation of multi-wavelength red laser output using cascaded diamond Raman oscillators pumped by a 532 nm laser and explore their output characteristics.

Methods　The setup of the multi-wavelength red diamond Raman laser is shown (Fig.1). The pump source is a self-built 532 nm frequency doubled nanosecond laser. The pump beam is collimated by the lens group F1 and F2. A half-wave plate (HWP) is used to adjust the polarization direction of the pump to be parallel to the <111> axis of the diamond crystal for the maximum Raman gain. The diamond Raman oscillator uses a plane-concave cavity with a curvature radius of 200 mm as the output mirror. The diamond size is 2 mm× 4 mm× 7 mm. The coating parameters of the two cavity mirrors are shown (Tab.1). The cavity mirrors are high reflection coated at first-order Stokes to increase the conversion efficiency and obtain pure higher-order Stokes output. The lens F3 is used to control the pump radius in the diamond crystal to about 350 μm. The total length of the Raman cavity is 60 mm, and the distance from the output coupler to the end surface of the diamond is 7 mm. The intrinsic modes

of the Raman cavity for each order of Stokes are shown (Fig.2), with a diamond between the purple dashed lines. The radius of the TEM_{00} modes of the first, second, third and fourth-order Stokes are 128, 133, 139, 146 μm, respectively.

Results and Discussions The spectra of second-order Stokes, second- and third-order Stokes, and second- to fourth-order Stokes were collected at pump energies of 343, 437, 1 165 μJ, respectively (Fig.3). The frequency shift between each Stokes order was 1 332 cm^{-1}, consistent with the inherent Raman frequency shift of diamond. With a maximum pump energy of 1 738 μJ (Fig.4(a)), three wavelength lasing in red with energies of 143, 425, 65 μJ were obtained, with slope efficiencies of 9.7%, 31.3%, and 8.7%, respectively. The conversion efficiency increases with pump energy and levels off (Fig.4(b)). A multi-wavelength red laser output energy of 633 μJ was obtained at a maximum pump energy of 1 738 μJ, with a slope efficiency of 45.3% and an optical-to-optical conversion efficiency of 36.4%. The temporal waveform of the incident pump at 532 nm and the output Stokes of each order at maximum pump energy were measured to be 11.43, 10.41, 3.75, 2.45 ns, respectively (Fig.5). The pulse width of each Stokes order is compressed compared to the pump, with more evident compression as the Raman order increases. The near-field spot of each Stokes order has no obvious distortion. The optical-to-optical conversion efficiency can be improved by optimizing the Raman cavity mode-matching degree, and the energy ratio of each wavelength in the multi-wavelength output can be controlled by designing the mirror coating.

Conclusions In this study, we developed a 532 nm pumped multi-wavelength diamond Raman laser and investigated its cascaded Raman laser output energy, spectrum, and pulse characteristics at different pump energies. Cascaded Raman outputs of 620, 676, and 743 nm were successfully demonstrated. With a maximum pump energy of 1 738 μJ, the output energies of 143 μJ at 620 nm, 425 μJ at 676 nm, and 65 μJ at 743 nm were achieved, with pulse widths of 10.41, 3.75, and 2.45 ns, respectively. Meanwhile, the near-field beams of all the orders exhibit good spatial distribution. The output energy of the combined multi-wavelength red laser was 633 μJ, with an optical-optical conversion efficiency of 36.4%. The results show that the visible light-pumped diamond Raman laser has tremendous potential for efficient all-solid-state miniaturized multi-wavelength lasers in red due to its extremely high Raman gain coefficient and excellent photothermal properties. This study can also provide guidance for the development of multi-wavelength Raman lasers pumped by other wavelengths.

Key words: Raman laser; diamond; multi-wavelength; pulse; high-power